Electron Transfer Rate Modulation in a Compact Re(I) Donor–Acceptor Complex

ARTICLE *in* DALTON TRANSACTIONS · JANUARY 2015

Impact Factor: 4.2 · DOI: 10.1039/C4DT02145B

7 AUTHORS, INCLUDING:

Yuankai Yue
Tulane University
7 PUBLICATIONS **25** CITATIONS
SEE PROFILE

Zheng Ma
Duke University
6 PUBLICATIONS **15** CITATIONS
SEE PROFILE

THE JOURNAL OF PHYSICAL CHEMISTRY B

Article

pubs.acs.org/JPCB

Evaluating the Extent of Intramolecular Charge Transfer in the Excited States of Rhenium(I) Donor–Acceptor Complexes with Time-Resolved Vibrational Spectroscopy

Yuankai Yue,[†] Tod Grusenmeyer,[†] Zheng Ma,[‡] Peng Zhang,[‡] Tri Tat Pham,[†] Joel T. Mague,[†] James P. Donahue,[†] Russell H. Schmehl,*[,†] David N. Beratan,*[,‡] and Igor V. Rubtsov*[,†]

[†]Department of Chemistry, Tulane University, New Orleans, Louisiana 70118, United States

[‡]Departments of Chemistry, Biochemistry, and Physics, Duke University, Durham, North Carolina 27708, United States

Supporting Information

ABSTRACT: Excited states in transition-metal complexes, even in those featuring ligands with strong electron donating and accepting properties, often involve only partial charge transfer between the donor and acceptor ligands. The excited-state properties of $[Re(bpy)(CO)_3L]^+$ compounds were studied, where L is 4-dimethylaminobenzonitrile (**Re4DMABN**), 3-dimethylaminobenzonitrile (**Re3DMABN**), and benzonitrile (**ReBN**) using time-resolved infrared (TRIR) and electronic spectroscopy methods as well as electronic structure computations. The DMABN complexes exhibit strongly solvent-dependent luminescence; the excited state lifetime decreases from microseconds in dichloromethane to several nanoseconds in mixed MeOH:DCM (1:1) solvent. Despite the similarities in the solvent dependence of the excited state dynamics and redox properties for **Re3DMABN** and **Re4DMABN**, the nature of the lowest energy excited states formed in these two compounds is drastically different. For example, the lowest energy excited state for **Re4DMABN** in the mixed solvent is assigned to the (4DMABN → bpy) ligand-to-ligand charge transfer (LLCT) state featuring partial charge transfer character. An equilibrium between a 3DMABN intraligand triplet (^{3}IL) and a metal-ligand-to-ligand charge transfer (MLLCT) state is found for **Re3DMABN** in the mixed solvent with the latter at ca. 400 cm^{-1} lower energy. The origin of such a drastic difference between the states involved in **Re4DMABN** and **Re3DMABN** is attributed to a difference in the energies of polarized quinoidal resonance structures in 4DMABN and 3DMABN ligands.

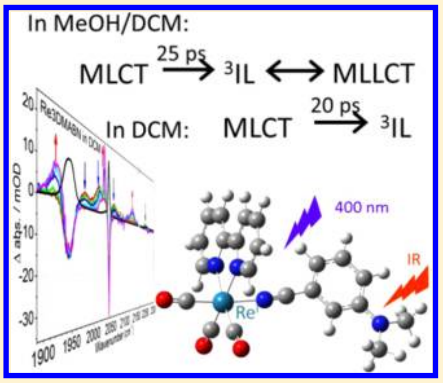

INTRODUCTION

The mechanism of photoinduced intramolecular electron transfer (ET) has been the subject of intensive study for more than 30 years.[1−7] Since photoinduced ET begins with light absorption, the electron-density distribution and degree of charge transfer associated with the initially formed and relaxed excited states are critical but are often poorly characterized. For transition metal complexes with metal-to-ligand charge transfer (MLCT) excited states, the structural and charge polarization changes that follow from the initial excitation to the generation of the intramolecular photoredox products can be subtle.[3,8,9] This is especially true when the free energy of the charge-separated state formed upon electron transfer is structurally similar to that of the initial excited state. Formation of an intramolecular charge-separated state may occur in discrete steps (i.e., initial formation of a MLCT excited state may be followed by an intramolecular electron-transfer step leading to polarization of charge from D to A) or absorption may directly create an excited electronic state with a significant admixture of the charge-separated DA product that then further relaxes. Distinguishing between these two closely related pathways requires a spectroscopic approach that provides direct temporal information on the electron-density distribution. The ability to evaluate the degree of state mixing using a direct spectroscopic approach may allow the correlation of the donor–acceptor interaction with the full course of the reaction on the excited state manifold.

Rhenium tricarbonyl–diimine complexes, $[Re^I(CO)_3(N,N)(L)]^{+/0}$ (+ when L is a neutral ligand with a substituent capable of electron donation to the excited complex), are appealing candidates to dissect the charge-transfer evolution as a function of time after excitation because infrared modes of the carbonyl and imine ligands provide direct probes of charge localization. Recent studies of Vlcek[10−14] and others provide insight into the vibrational relaxation of the MLCT states of $[Re^I(CO)_3(N,N)(L)]^{+/0}$ complexes, where L = pyridine or chloride. In these complexes, the lowest energy metal to ligand charge transfer (MLCT) state is directly or indirectly prepared by optical

Special Issue: Michael D. Fayer Festschrift

Received: September 26, 2013
Revised: October 12, 2013
Published: October 13, 2013

excitation.[13,15−18] Picosecond time-resolved changes in the CO stretching mode frequencies of the complexes indicate that formation of the vibrationally relaxed ^{3}MLCT state in halocarbon solvents occurs with time constants in the range of 1−10 ps. Vleck and others used ps time-resolved infrared (TRIR) spectroscopy to follow the dynamics of intramolecular energy and electron transfer in rhenium carbonyl systems with well-defined charge-separated states.[19−24]

In the regime of small driving force, light-induced ET dynamics can be controlled by the solvent medium. Using time-resolved UV−vis methods, Schanze and co-workers explored the photophysics of $[(bpy)Re^{I}(CO)_3(4DMABN)]^+$ (4DMABN = 4-dimethylaminobenzonitrile) in solvents ranging from pure methylene chloride (DCM) to pure acetonitrile (AN) in polarity. Luminescence results indicated strong, long-lived (∼1 μs) emission from the complex in DCM, and comparisons to $[(bpy)Re^{I}(CO)_3(AN)]^+$ indicated that the emitting excited-state is a Re(dπ) to bpy(π*) MLCT state. Increasing the mole fraction of acetonitrile in mixed solvents caused the emission quantum yield to decrease nearly to zero and caused the lifetime to decrease to less than 1 ns for the 4DMABN complex. This behavior was attributed to the formation of a 4DMABN to bpy interligand charge transfer (LLCT) state ($[(bpy^-)Re^{I}(CO)_3(4DMABN^+)]^+$) that rapidly relaxes to the ground state. The LLCT state was postulated to form via initial excitation of a MLCT state followed by intramolecular electron transfer to produce the LLCT state. The relative energies of the MLCT and LLCT states were suggested to interchange on changing the solvent from DCM to DCM/AN mixtures. The observed behavior (including ps time-resolved visible spectroscopy) is consistent with the model.[23]

Here, we use time-resolved infrared (TRIR) and UV−vis spectroscopies as well as DFT and TDDFT computations to probe $[(bpy)Re^{I}(CO)_3(4DMABN)]^+$ (**Re4DMABN**) and the related complex with a 3-dimethylamino-benzonitrile ligand (**Re3DMABN**) (Scheme 1). The results indicate that, despite similarity of the redox properties of the two complexes and their excited-state lifetime solvent dependence, the nature of the excited states involved differs drastically. For example, in DCM, **Re4DMABN** has a metal−ligand (Re−4DMABN) to ligand (bpy) MLLCT state, while the ^{3}IL state is lowest in energy for **Re3DMABN**. In MeOH/DCM (1:1) mixed solvent, the lowest energy state for **Re4DMABN** is (4DMABN → bpy) LLCT, although it is a MLLCT state for **Re3DMABN**. Definitive assignment was only possible by considering all available data, which include TRIR spectral data with numerous IR labels, fluorescence lifetime measurements, triplet quenching results, and DFT computations. A simple three-state coupling model is presented to describe the states formed in both compounds in the two solvent systems.

Scheme 1. Structures of the ReBN, Re4DMABN, and Re3DMABN Compounds

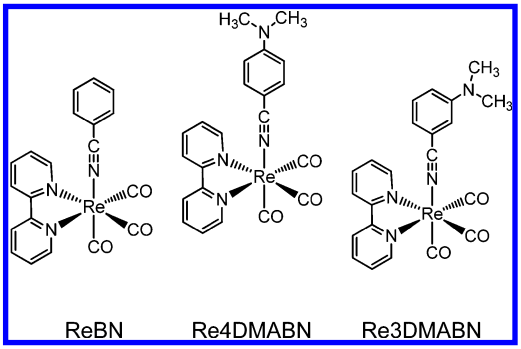

EXPERIMENTAL DETAILS

Complex Synthesis and Sample Preparation. Toluene, methylene chloride, and hexane were purchased from PHARMCO-AAPER. $[Re(CO)_5Cl]$ was purchased from Strem Chemical. 3-Aminobenzonitrile, 2,2′-bipyridine, paraformaldehyde, and sodium cyanoborohydride were purchased from Sigma Aldrich. Benzonitrile and 4-dimethylaminobenzonitrile were purchased from Alfa Aesar. All synthetic materials were used as received other than 3-aminobenzonitrile which was *N*-methylated using a published literature method.[25] The complexes $[Re(bpy)(CO)_3(L)]$ (BArF) (L = BN, 3DMABN, 4DMABN; BArF = tetrakis(3,5-bis(trifluoromethyl)phenyl)-borate) were prepared according to modifications of literature methods.[25−27] The purity of the compounds was evaluated by ^{1}H NMR and MALDI TOF mass spectrometry. In addition, structures were obtained for all three complexes by single crystal X-ray diffraction, and CIF files are provided as Supporting Information. Synthetic details, NMR spectra, MALDI spectra, and ORTEP representations are provided in the Supporting Information. NMR spectra were recorded on a Varian 400 MHz NMR spectrometer. MALDI spectra were obtained on a Bruker Autoflex III time-of-flight mass spectrometer. All UV−vis absorption spectra were measured on a Hewlett-Packard 8452 diode array spectrophotometer. Luminescence spectra were obtained using a PTI scanning spectrofluorimeter.

Sample solutions for transient infrared experiments: solutions of 20 mM concentration were prepared in two solvents: pure dichloromethane (DCM) and methanol/DCM mixture (1:1 by volume), referred to here as MeOH/DCM solvent. The spectroscopic grade solvents (Aldrich) were used as received. To avoid influence of sample degradation over laser excitation, the time-resolved measurements were performed in a flow cell (DLC2, Harrick) with an optical path length of 150 μm at 23.5 ± 0.5 °C. A sample solution of ca. 2.5 mL was circulated by a micro-annular gear pump (mzr-2942, HNP Mikrosysteme). The IR spectra of the sample before and after the experiment differ by less than 10%.

Cyclic Voltammetry. Voltammograms were obtained using a CH Instruments CH1730A Electrochemical Analyzer. The working electrode was a glassy-carbon electrode, the counter electrode was a Pt wire, and the reference electrode was an aqueous Ag/AgCl electrode. Data were collected in acetonitrile and dichloromethane solutions containing 0.1 M $TBAPF_6$. All samples were bubble degassed with argon for 10 min prior to collection.

Femtosecond Time-Resolved Spectroscopy. A three-pulse (UV/IR/Vis) experimental setup, capable of performing fs time-resolved infrared spectroscopy (TRIR), fs transient absorption spectroscopy (TA), and IR-perturbed transient absorption spectroscopy, has been built.[28] A laser beam at 804 nm produced by a Ti:sapphire oscillator and regenerative amplifier featuring pulses of 44 fs duration and 1.1 mJ energy at 1 kHz repetition rate was split into three parts. One part of ca. 630 μJ/pulse was frequency doubled to generate 402 nm excitation pulses. After passing a 150 mm long delay stage (NRT150, Thorlabs), it was focused into the sample with a 300 mm focal length lens. The second part of the fundamental beam of ca. 370 μJ/pulse was used to pump an in-house built

dx.doi.org/10.1021/jp409628e | J. Phys. Chem. B 2013, 117, 15903−15916

Table 1. Selected Bond Lengths (Å) and Bond Angles (deg) Obtained from Single Crystal Structures of the [Re(bpy)(CO)$_3$L](BArF) Complexes

	Re4DMABN	Re3DMABN	ReBN
Nitrile Information			
Re−N (nitrile) bond length	2.134(4)	2.124(2)	2.108(8)
CN bond length	1.144(6)	1.150(3)	1.14(1)
C(phenyl)−C(nitrile) bond length	1.424(6)	1.435(3)	1.43(1)
C(phenyl)−N(dimethyl) bond length	1.363(6)	1.372(4)	
Re−N−C (nitrile) angle	174.3(3)	177.7(2)	178.3(8)
Bipyridine Information			
average Re−N(bpy) bond length	2.167(3)	2.171(2)	2.172(7)
CO Information			
CO (trans to nitrile) bond length	1.142(5)	1.151(3)	1.12(1)
Re−C (CO trans to nitrile) bond length	1.917(4)	1.930(2)	1.95(1)
average CO (trans to bpy) bond length	1.143(6)	1.149(4)	1.15(1)
average Re−C (CO trans to bpy) bond length	1.928(5)	1.929(3)	1.93(1)

optical parametric amplifier (OPA), which produces signal-idler pulse pairs. The signal-idler beam was focused into a 1.5 mm thick $AgGaS_2$ crystal to generate mid-IR pulses through a difference frequency generation process. The mid-IR beam was focused into the sample cell with a lens of 100 mm focal length. The third part of the 804 nm beam (ca. 7 μJ/pulse) was delayed by a delay stage of 600 mm long (Parker), intensity-tuned by a wave plate-polarizer pair, and focused into a 1 mm thick sapphire wafer with a 100 mm lens to generate white light continuum. The white light was then focused into the sample using a 40 mm achromatic lens.

The TRIR measurements described here were made using excitation pulses at 402 nm of 2−3 μJ pulse energy and mid-IR probe pulses. The spot diameters of the pump and probe beams in the sample were ca. 150 and 100 μm, respectively, measured at half of the beam power. The fraction of the excited molecules in the experiment was ca. 1−1.5%, calculated on the basis of the ratio of transient absorption in ν(CO) bleach peaks and their linear absorption. Such excitation fraction corresponds to preparing ca. 1.0−1.5% of doubly-excited species of all excited molecules. After passing through the sample, the mid-IR probe pulses were dispersed in a monochromator (TRIAX-190, HORIBA) and measured by a single-channel MCT detector (MCT-11-1.00, Infrared Associates). The polarizations of the pump and probe pulses in the experiments were perpendicular to each other. The anisotropy induced by a 402 nm excitation is rather small, indicating that several electronic transitions are excited (see the Supporting Information). The mid-IR pulses are tunable from 1100 to 4000 cm^{-1} and have a spectral width of ca. 200 cm^{-1} (fwhm). A spectra resolution of 1 cm^{-1} was achieved.

Nanosecond Spectroscopy. Transient absorption spectra in the UV and visible spectral regions were obtained by collecting transient decays at 10 nm intervals following pulsed laser excitation using a system involving an Applied Photophysics LKS 60 optical system/software and a Quantel Brilliant laser equipped with second and third harmonics and an OPOTEK OPO (420−670 nm) for tunable excitation. The excitation wavelength used for these complexes was 420 nm. Samples were degassed with N_2 for 20 min prior to acquisition of transient decays.

Quantum Chemistry Calculations. Calculations on the electronic ground states and the lowest energy triplet states of three related rhenium complexes were performed using hybrid B3LYP density functional theory (DFT). Characterization of low-lying singlet and triplet excited states (at Franck−Condon geometries and optimized geometries on the potential energy surfaces) and normal-mode analyses were carried out using time-dependent density functional theory (TDDFT). 6-31G** basis sets were used for C, H, O, and N atoms. The LANL2DZ relativistic effective core potential and associated basis set were used for rhenium. The polarizable continuum model was employed to describe the solvent effects in the ground-state and excited-state calculations. All the quantum chemical calculations were performed using the Gaussian 09 software package.[29] Four types of charge-population analysis were performed, including Mulliken charge, Löwdin charge, NBO charge, and the charge population acquired from electrostatic potential fitting (ESP charge), to determine the charge distributions of the corresponding electronic states. For all calculations, these four types of charge population analysis give qualitatively consistent results. Therefore, only the result of Mulliken charge presented and discussed.

RESULTS AND DISCUSSION

Synthesis and Structural Characterization. The complexes studied were readily prepared using [(bpy)-Re^{I}(CO)$_3$(OTf)] (OTf = triflate) by reaction with the benzonitrile ligand and metathesis of the resulting triflate salt with NaBArF, precipitating sodium triflate. Synthetic details, characterization of the complexes, including proton NMR, MALDI mass spectra, and single crystal structure data, are provided in the Supporting Information. Crystal structures of the three complexes indicate only small differences among them in bond distances (<20 pm) and angles for the Re, CO ligands and bpy ligand; selected bond distances and angles are given in Table 1. The three benzonitrile ligands (BN, 3DMABN, and 4DMABN) also exhibit only minor differences in the Re−N and NC bond lengths; the bond angles and lengths in the phenyl ring also change very little among the three complexes. For both DMABN ligands, the Re−N (nitrile) bond length is slightly longer than that for the BN ligand. This observation, taken together with the fact that the bond length of the Re−C (CO) *trans* to the DMABN ligand is shorter than that for the BN complex and the *trans* CO bond length is longer, suggests that electron donation from the dimethylamine substituent diminishes the Re−nitrile back bonding interaction and increases the backbonding to the *trans* CO in the electronic ground state. This trend is also reflected in the infrared spectra of the complexes (*vide infra*).

dx.doi.org/10.1021/jp409628e | J. Phys. Chem. B 2013, 117, 15903−15916

UV−vis Absorption Spectra, Luminescence Spectra, and Transient Absorption. Figure 1 shows that the UV−vis absorption spectra of **ReBN** and **Re3DMABN** in dichloromethane (DCM) have maxima at ca. 320 nm that are assigned to bpy-localized $\pi-\pi^*$ transitions,[30] while **Re4DMABN** has a unique strong absorption at 334 nm with a relatively high molar absorptivity that, by comparison with the 4DMABN ligand, is clearly an intraligand amine to nitrile charge transfer transition (ILCT).[30] Weaker broad absorption transitions from 320 to 430 nm were assigned to $d\pi(Re) \rightarrow \pi^*(bpy)$ MLCT transitions based on earlier observations.[18,31−33] Vertical excitation calculations using TDDFT predicted that the MLCT transitions are at ca. 379, 372, and 385 nm in **ReBN**, **Re4DMABN**, and **Re3DMABN**, respectively. For **Re4DMABN**, the vertical excitation energies of S1, S2, T1, and T2 are 476, 372, 481, and 441 nm, respectively. The nature of these states at the Franck−Condon geometry are LLCT, MLCT, LLCT, and ILCT, respectively. The oscillator strength of S2 is 0.0137, while that of S1 is 0.0020. For **Re3DMABN**, the vertical excitation energies and nature of the states for S1, S2, T1, and T2 are 494 nm (LLCT), 387 nm (ILCT), 514 nm (LLCT), and 494 nm (ILCT), respectively. The MLCT states according to TDDFT calculations are from S3 to S5 with energies of 385, 361, and 352 nm, and the corresponding oscillator strengths are 0.0043, 0.0894, and 0.0531. The oscillator strengths of S1 and S2 are 0.0001 and 0.0748. The computed electronic spectrum agrees well with experiments.

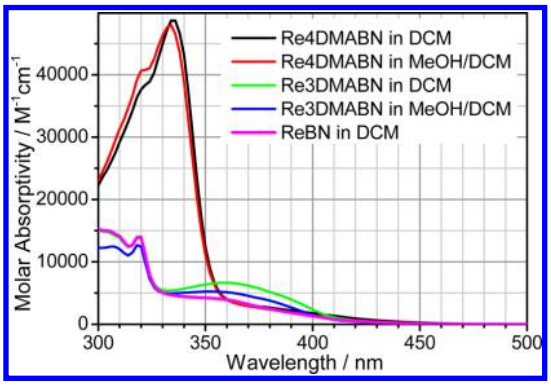

Figure 1. Absorption spectra of the three complexes in DCM and MeOH/DCM.

All three complexes exhibit luminescence in DCM at room temperature, and spectra are shown in Figure 2 for emission in DCM and MeOH:DCM (1:1). Emission maxima, luminescence quantum yields, and excited state lifetimes are given in Table 2. On the basis of previous literature reports[23] and computational results described here (*vide infra*), the yellow luminescence from the **ReBN** complex is from the $Re(d\pi) \rightarrow bpy(\pi^*)$ MLCT state. The similarity of the observed emission maximum and line shape of the DMABN complexes suggest that the emission originated in MLCT transitions. However, the 3DMABN complex differs from the other two in that the emission is very weak in DCM. A striking feature of **Re3DMABN** is that the lifetime of the weak luminescence is more than a factor of 30 longer than the measured lifetime of the other two complexes. This very long-lived and weak luminescence suggests that the emitting excited state is *not* MLCT in origin. The possibility of impurity luminescence in the 3DMABN complex can be ruled out by the observation of a long-lived transient absorption (Figure 3); the **Re3DMABN** purification is discussed in the Supporting Information.

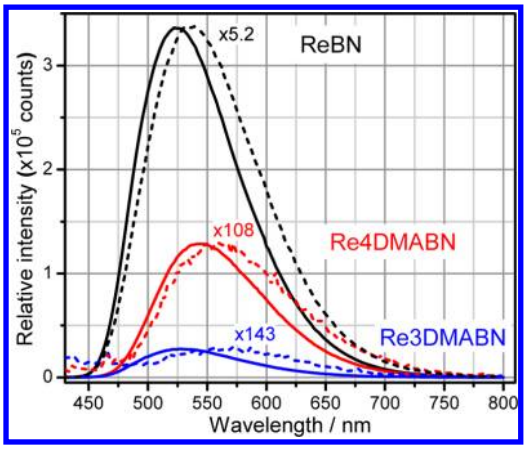

Figure 2. Luminescence spectra of the complexes in aerated DCM (solid lines) and in MeOH/DCM (dashed lines) at room temperature. The spectra in MeOH/DCM were scaled to match those in DCM by the factors indicated in the inset.

All of the complexes have excited state UV−vis absorbance between 400 and 450 nm, which parallels the results of Schanze et al. for **Re4DMABN** in mixed DCM/CH_3CN solutions.[23] The BN and 4DMABN complexes exhibit bleaching at longer wavelengths that results from the luminescence of these complexes. Despite similarities among the transient spectra of the long-lived states in the three compounds (Figure 3), it is very likely that the equilibrated excited state of the **Re3DMABN** complex differs from the others, since its radiative decay rate (Table 2) is nearly a factor of 1000 slower than the BN and 4DMABN complexes.

Upon changing the solvent to the more polar MeOH/DCM (1:1) mixture, all of the complexes exhibit weaker luminescence and shorter excited state lifetimes. The magnitude of the change is much more pronounced in the two DMABN complexes. In the two DMABN complexes, the luminescence and transient absorbance lifetimes decrease by a factor of >100 in the mixed solvent, as compared to a factor of 1.6−3 for **ReBN**. In **Re3DMABN**, the excited state lifetime in DCM is more than 30 times longer than that of either of the other complexes but decreases precipitously in the mixed solvent, from 25 to 30 μs in DCM to 30 ns in MeOH/DCM. The **ReBN** and **Re3DMABN** transient spectra in MeOH/DCM were essentially the same as those in DCM, with shorter lifetimes, as reported in Table 2. Such excited state lifetime decreases in more polar solvents are often associated with the existence of strongly polarized excited states, which are higher in energy in non-polar solvents but are stabilized in polar solvents and provide additional relaxation pathways to the ground state. Such polarized states could be either ligand-to-ligand charge separated states (LLCT), $[(bpy^-)Re(CO)_3(DMABN^{+\bullet})]^+$, or highly polarized ligand-based states.

Electrochemistry. Cyclic voltammetry measurements on the complexes exhibit waves attributable to one-electron reduction and oxidation in DCM and CH_3CN solutions (Table 3; CVs included in the Supporting Information). Here, CH_3CN was used in place of CH_3OH, since it was not possible to obtain voltammetric data in CH_3OH because of competing solvent redox processes. The observed waves at positive potentials in the voltammograms of both of the DMABN complexes occur more than 0.5 V more negative than the first

dx.doi.org/10.1021/jp409628e | J. Phys. Chem. B 2013, 117, 15903−15916

Table 2. Luminescence Maxima, Quantum Yields, and Lifetimes of the Complexes in Aerated DCM and MeOH/DCM (1/1) at Room Temperature

complex	ReBN		Re3DMABN		Re4DMABN	
solvent	DCM	MeOH/DCM	DCM	MeOH/DCM	DCM	MeOH/DCM
luminescence λ_{max} (nm)	524	536	528	565	544	560
luminescence quantum yield	0.41	0.10	0.003	<0.001	0.17	0.002
luminescence lifetime (μs)	1.33 ± 0.05	0.78 ± 0.05	35.0 ± 1.5 (88%) 1.26 ± 0.1 (12%)	0.57 ± 0.05 (73%) 0.04 ± 0.01 (27%)	0.84 ± 0.02	
transient absorption lifetime (μs)	1.35 ± 0.1	0.78 ± 0.09	23.3 ± 1.0 0.78 ± 0.02	0.03 ± 0.01	0.81 ± 0.07	
k_r (s^{-1})	3.1×10^5	1.3×10^5	130		2.0×10^5	
k_{nr} (s^{-1})	4.4×10^5	1.1×10^6	5.0×10^4		1.0×10^6	

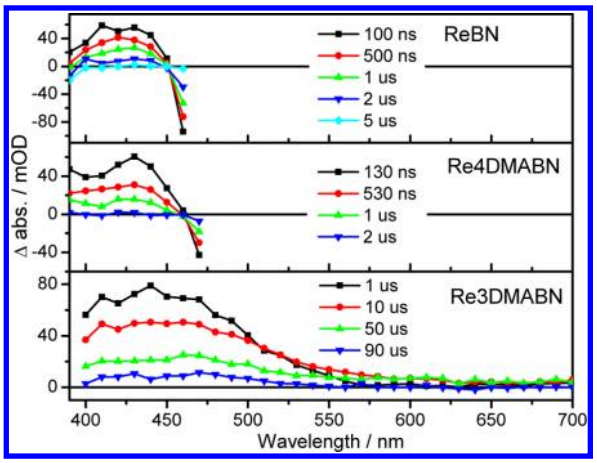

Figure 3. Nanosecond transient absorption spectra of **ReBN**, **Re3DMABN**, and **Re4DMABN** in DCM at room temperature at the delay times indicated. Strong luminescence observed for the **ReBN** and **Re4DMABN** complexes in the 480−690 nm range is not shown (appearing as negative absorbance).

oxidation of the **ReBN** complex (E^0(Re(II)/Re(I)), and are clearly associated with oxidation of the dimethylamine substituent.[34] The oxidation is quasi-reversible in acetonitrile, suggesting that the cation radical reacts irreversibly within a few seconds of being formed (sweep rates were 0.1 V s^{-1}). In addition, oxidation in DCM is observed at more positive potentials than in CH_3CN. Reductive voltammograms in CH_3CN are reversible, and reductive waves occur at nearly the same potential for all three complexes. The reductive behavior in DCM is irreversible, but cathodic peaks are clearly observed for both DMABN complexes. These data are included in Table 3. The difference between E^0(2+/+) and E^0(+/0) provides an approximate value for the energy of the charge separated species, [(bpy$^-$)Re(CO)$_3$(DMABN+•)]; the values of ΔE_{CS}, shown in Table 3, are well in excess of 2 V, suggesting that back electron transfer from this state may reside in the Marcus inverted region. The emission maxima have energies at least 0.1 V lower than the estimated charge-separated states in each case, and while the true excited state energies will be somewhat higher, it is clear that the free energies for intramolecular electron transfer reaction will be close to zero.

Infrared Absorption Spectra. Vibrational absorption spectra of the three compounds feature several characteristic peaks that are readily assigned (Figure 4, Table 4). The

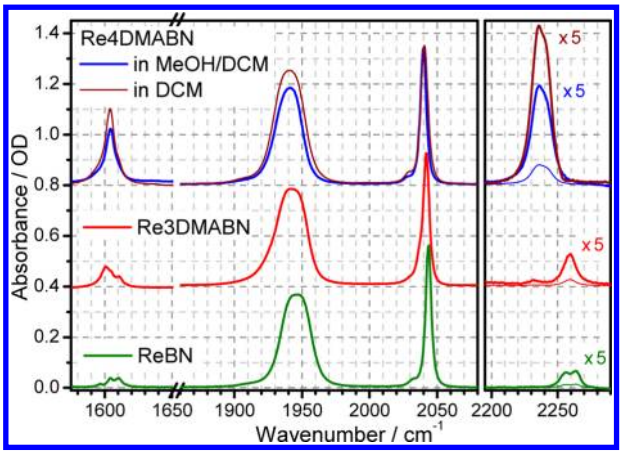

Figure 4. Linear absorption spectra of the three compounds in DCM and MeOH/DCM. The baselines for two of them are shifted by 0.4 and 0.8 for clarity. The spectra in the right panel were scaled by 5-fold (thick lines), while thin lines show unscaled spectra.

strongest peaks at ca. 2040 and ca. 1945 cm^{-1} belong to the symmetric and asymmetric stretching modes of the three carbonyl ligands, respectively.[22] Notice that the much broader peak at ca. 1945 cm^{-1} consists of two ν_{as}(CO) transitions.[22] The relatively weak peak around 2250 cm^{-1} belongs to the C≡N stretching mode. Two additional peaks of interest are apparent in the 1600−1615 cm^{-1} region for all three compounds. DFT calculations indicate that the two vibrational transitions between 1600 and 1615 cm^{-1} correspond to the symmetric ring stretching mode of the bpy, ν_{ss}(bpy), and a stretching motion of the phenyl ring of DMABN (or BN), ν_{ss}(Ph) (Table 4). The weaker absorption peak, that appears at

Table 3. Redox Potentials (in V) for the Complexes in DCM and CH_3CN vs Ag/AgCl and Free Energies of the Charge Separated States

complex	E^0(2+/+), (ΔE_p, V) in DCM	E^0(2+/+), (ΔE_p, V) in CH_3CN	E(+/0), in DCM	E^0(+/0), (ΔE_p, V) in CH_3CN	ΔE_{CS}, V in DCM (in CH_3CN)
[(CO)$_3$Re(bpy)(BN)]$^+$	>1.5	>1.7			
[(CO)$_3$Re(bpy)(3DMABN)]$^+$	1.28 (0.24)	1.17 (0.14)	−1.13	−1.17 (0.08)	2.41 (2.34)
[(CO)$_3$Re(bpy)(4DMABN)]$^+$	1.43 (0.09)	1.27 (0.07)	−1.16	−1.16 (0.08)	2.59 (2.43)

dx.doi.org/10.1021/jp409628e | J. Phys. Chem. B 2013, 117, 15903−15916

Table 4. Experimental and DFT Computed Ground State Vibrational Frequencies (in cm^{-1}) of Several Characteristic Modes for the Three Compounds in DCM

ReBN		Re4DMABN		Re3DMABN		
exper.	DFT, GS (Δ)	exper.	DFT, GS (Δ)	exper.	DFT, GS (Δ)	assignment
2260	2340 (80)	2236	2316 (80)	2260	2344 (84)	ν(C≡N)
2043	2105 (62)	2040	2100 (60)	2042	2100 (58)	ν_{ss}(CO)
1946[a]	2010 (64)	1941[a]	1999 (58)	1942[a]	2003 (61)	ν_{as}(CO), as_2
	2000 (54)		1994 (53)		1997 (55)	ν_{as}(CO), as_1
1612	1651 (39)	1611	1651 (40)	1612	1651 (39)	ν_{ss}(bpy)
1604	1648 (44)	1604	1653 (49)	1601	1647 (46)	ν_{ss}(Ph)

[a]While the presence of two peaks is apparent in the spectra, no attempts were made to deconvolute them.

approximately a constant frequency of 1612 cm^{-1}, is assigned to ν_{ss}(bpy), while the lower-frequency peak at ca. 1604 cm^{-1} has different IR intensities in the different compounds (Table 4 and Table S1, Supporting Information), and is assigned as ν_{ss}(Ph). The DFT calculations suggest only a minor mixing of these two modes that does not exceed ~5%. Interestingly, not only is the ν_{ss}(Ph) peak in **Re4DMABN** much stronger than that of ν_{ss}(bpy), but its extinction coefficient is comparable to that of the ν(CO) transitions. Note that the ν_{ss}(Ph) mode involves symmetric stretching motion of the phenyl ring along the long axis of the ligand and its IR intensity is strongly dependent on the ligand polarization.

The stretching frequency of the metal coordinated CO is known to be sensitive to the metal center's charge,[17,20] a result of π backbonding from the metal influencing the CO bond order. The fact that the CO absorption peaks for these complexes show only small differences in both their central frequencies and their IR intensities suggests that the ground state charge of Re is similar in all three complexes.

Larger differences between the three complexes are found in the C≡N stretching region. While the CN frequencies for **ReBN** and **Re3DMABN** are similar, there is a striking 24 cm^{-1} shift of ν(CN) to lower frequencies in **Re4DMABN**. In addition, the IR intensity of ν(CN) in **Re4DMABN** is more than 3-fold larger than in the other complexes. These differences suggest that the 4DMABN ligand, but not 3DMABN or BN, significantly affects the electron density distribution in the complex's ground electronic state. The main electron distribution differences occur in the L-ligand region and on the neighboring groups, as can be seen from the Re−N (nitrile) and Re−C (CO trans to nitrile) bond lengths as well as from the Re−N−C angle (Table 1). This is further supported by the DFT computations (Table 5).

Transient Infrared Spectroscopy. In an effort to understand the differences in the characteristics of the excited states for the three complexes, TRIR spectra were measured in the spectral regions of the CO (1900−2150 cm^{-1}), CN (2150−2310 cm^{-1}), and ring (1540−1640 cm^{-1}) vibrations. The transient spectra represent the differences between the vibrational spectra in the excited and ground electronic states; positive peaks belong to absorption by modes of the excited states and negative peaks are due to bleaching of ground electronic state modes. TRIR spectra in the CO stretching region were previously reported for a variety of rhenium tricarbonyl[15−17,20,35,36] and other transition metal complexes, and a general understanding of the associated spectral changes has been reached. Removal of electron density from the metal in Re-to-bpy MLCT transitions leads to a decrease of the Re(dπ) backbonding to the π^* orbitals of CO ligands and to an increase of the CO stretching frequencies.[37] Conversely, decreases of the CO frequencies indicate an increase of electron density at the metal.

Table 5. Calculated Mulliken Charges for the Ground State (S0) and the Lowest Energy Triplet State (T1) in DCM and in Water and the Charge Changes (T1−S0)

functional group	in DCM			in water		
	S0	T1	T1−S0	S0	T1	T1−S0
ReBN						
bpy	0.53	0.27	−0.26	0.53	0.34	−0.19
BN	0.19	0.21	+0.02	0.19	0.21	+0.02
Ph	0.37	0.39	0.02	0.37	0.38	0.01
CN	−0.18	−0.18	0.00	−0.18	−0.17	0.01
Re	0.63	0.73	+0.10	0.63	0.71	+0.08
3 CO	−0.35	−0.21	+0.14	−0.35	−0.26	+0.09
Re3DMABN						
bpy	0.52	0.50	−0.02	0.53	0.51	−0.02
3DMABN	0.18	0.28	+0.10	0.20	0.30	+0.10
DMA	0.52	0.72	+0.20	0.53	0.73	+0.20
Ph	−0.14	−0.09	+0.05	−0.14	−0.08	+0.06
CN	−0.20	−0.35	−0.15	−0.19	−0.35	−0.16
Re	0.62	0.60	−0.02	0.63	0.61	−0.02
3 CO	−0.34	−0.40	−0.06	−0.36	−0.42	−0.06
Re4DMABN						
bpy	0.52	−0.15	−0.67	0.53	−0.20	−0.73
4DMABN	0.22	0.64	0.42	0.22	0.82	0.60
DMA	0.00	0.17	0.17	0.00	0.24	0.24
Ph	0.45	0.70	0.25	0.45	0.78	0.33
CN	−0.23	−0.23	0.00	−0.22	−0.2	0.02
Re	0.62	0.73	0.11	0.62	0.70	0.08
3 CO	−0.36	−0.23	0.13	−0.37	−0.31	0.06

ReBN in DCM: Long-Lived MLCT State Is Formed. The TRIR of **ReBN** in DCM is shown in Figure 5. The early time transient spectra of the CO modes following 402 nm excitation of **ReBN** are characteristic of MLCT state formation.[37] The two ν_{as}(CO) peaks that overlap in the ground state are well resolved in the excited state, with the maxima at small delay times of 1976 and 2017 cm^{-1}. The large frequency increase of all three CO peaks observed instantaneously upon excitation, +64 (as_1), +30 (as_2), and +11 cm^{-1} (ss), is in accord with formation of a Re(dπ) → (π^*)bpy MLCT state. (The dynamics occurring faster than the instrument response time of ca. 200 fs is described as instantaneous.) The excited state absorption peaks show dynamics with a characteristic time of ca. 17 ps (Figure 5), which results in a further shift to higher frequencies of all three CO peaks by +5 (as_1), +6 (as_2), and +2.5 cm^{-1} (ss), peak narrowing, as well as growth of the ν_{ss}(CO) and ν_{as1}(CO) peak amplitudes (Figure 5 and Table S2, Supporting

dx.doi.org/10.1021/jp409628e | J. Phys. Chem. B 2013, 117, 15903−15916

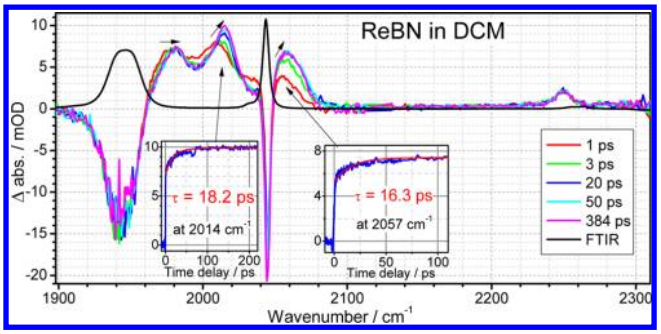

Figure 5. Time-resolved IR spectra of **ReBN** in DCM following 402 nm excitation. Insets show kinetics measured at indicated frequencies and their fits to a single exponential function. The arrows indicate the directions of the spectral changes in the excited state.

Information). Importantly, the excited state relaxation does not lead to recovery of the ground electronic state vibrational frequencies, as the bleaching peaks do not diminish in intensity. Such dynamics can be assigned to a combination of solvation, vibrational cooling, and electronic relaxation among different excited states.[20,38,39] There is considerable evidence in the literature to indicate that the electronic relaxation to the lowest triplet MLCT state in complexes with heavy metals such as Re occurs within several hundred femtoseconds.[12,35] The solvation process in DCM is very fast with the slowest solvation component reported at 1.0 ps.[40] Thus, vibrational cooling remains the most likely cause of the observed dynamics.[20] Vibrational relaxation to the lowest MLCT state following 402 nm excitation deposits ca. 6000 cm^{-1} (using the luminescence peak at 524 nm) of excess energy into the complex within the first few hundred femtoseconds after excitation, resulting in excitation of a range of vibrational modes in the complex. Anharmonic coupling of these modes with the CO modes causes frequency shifts of the latter.[38,39,41−43] Thus, cooling of the complex causes the CO peaks to narrow and shift to higher frequencies. A thermalization time in a non-polar solvent under similar concentration and excitation conditions was previously found to be ca. 20 ps using relaxation-assisted 2DIR spectroscopy.[41] The CO modes are clearly the most sensitive to the excess energy, possibly because of a large dipole−dipole contribution to their interaction energy with the other modes in the complex.

There is a small instantaneous shift of the CN mode frequency of ca. −10 cm^{-1} upon electronic excitation; in addition, the CN transition dipole in the excited state increases ∼4-fold. Apparently, the ps excited state dynamics affecting the CO modes does not perturb the CN mode, confirming that the BN ligand is not involved significantly in the MLCT transition and that the ground state backbonding to the CN is much less than that for the CO ligands. Results of DFT calculations support the formation of the Re(dπ) → bpy(π^*) transition. The calculated changes in Mulliken charges (Table 5) between the ground and excited states indicate little change on the

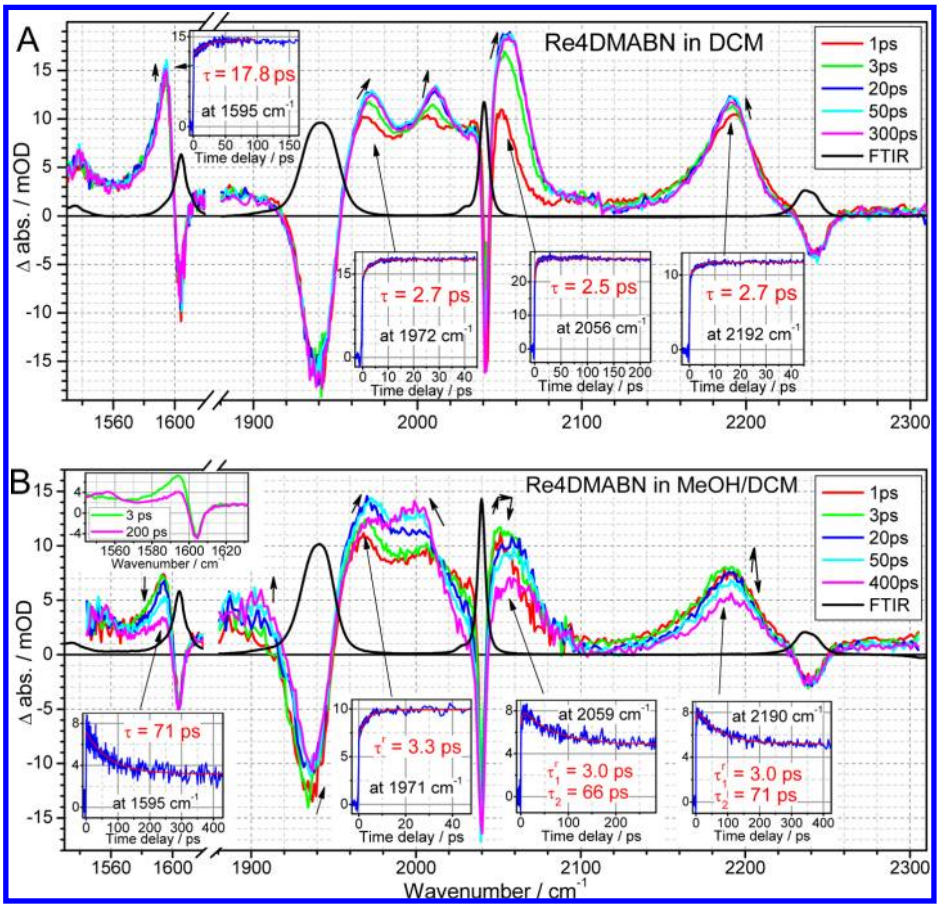

Figure 6. Time-resolved IR spectra of **Re4DMABN** in (A) DCM and (B) MeOH/DCM following 402 nm excitation. Insets show kinetics measured at indicated frequencies together with a single exponential fit (if two time components are shown). The arrows indicate the directions of the spectral changes in the excited state.

dx.doi.org/10.1021/jp409628e | J. Phys. Chem. B 2013, 117, 15903−15916

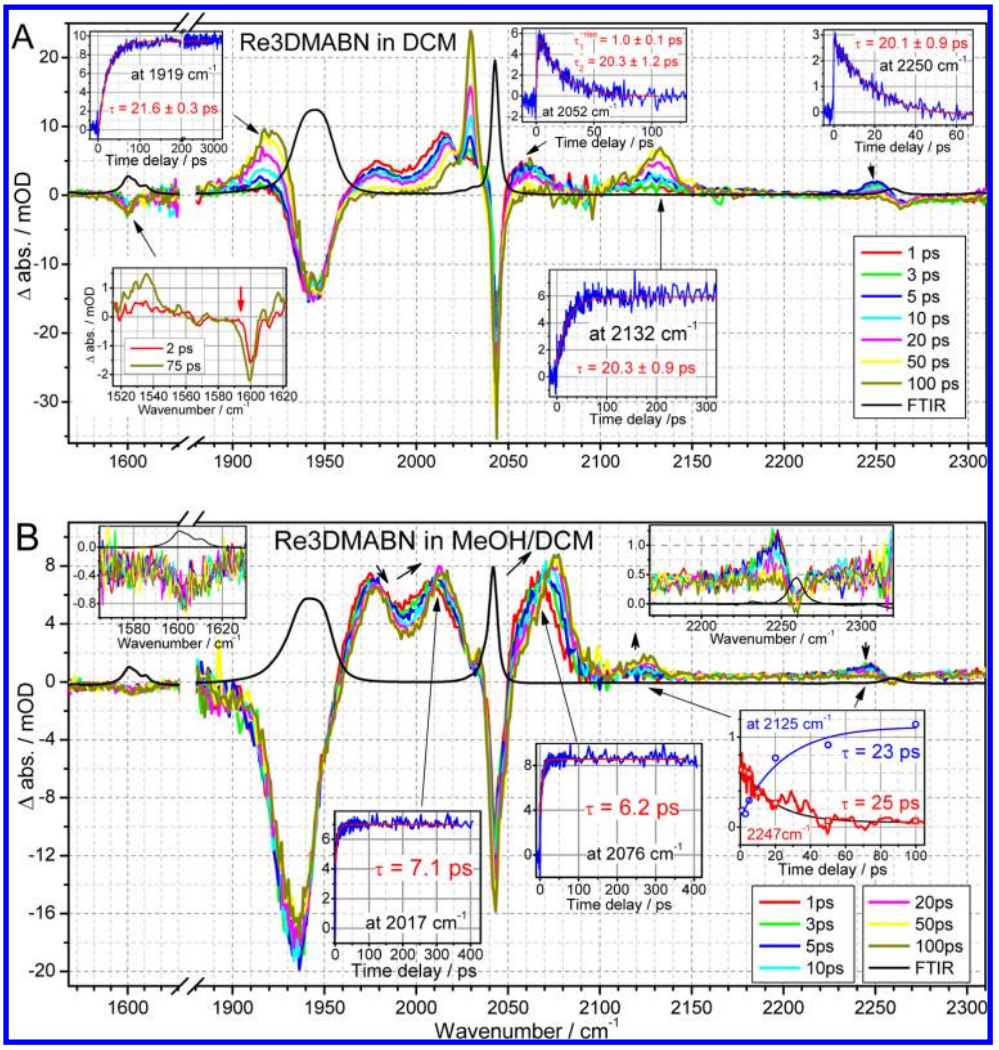

Figure 7. Time-resolved IR spectra of **Re3DMABN** in (A) DCM and (B) MeOH/DCM following 402 nm excitation. The insets show kinetics and zoomed in transient spectra.

nitrile ligand, as well as the formation of a positive charge on the Re and CO ligands and negative charge on the bpy. No further spectral changes beyond 50 ps are found for **ReBN** in the 430 ps time window; the overall excited state lifetime of ~0.8 μs is attributed to the lifetime of the MLCT state of **ReBN**.

Re4DMABN in DCM: Despite Long Lifetime, the Lowest Energy Excited State Is Different than in ReBN. The TRIR spectra of **Re4DMABN** in DCM in the CO region are similar to those of **ReBN**, implying that a similar MLCT state is formed upon excitation (Figure 6A and Table S2, Supporting Information). However, in contrast to **ReBN**, the CN mode in **Re4DMABN** decreases in frequency by 46 cm^{-1} in the excited state and exhibits a large increase in intensity, indicating a change of the CN bond order toward a double bond limit. Assuming that the stretch at this frequency is truly CN localized in both ground and excited states, the ratio of the ground to excited state force constants is 1.04; computational results yield different values of the absolute stretching frequencies (Table S3, Supporting Information), but the relative change in the force constant is the same for both the S1 and T1 states. In addition, the ν_{ss}(Ph) peak at 1604 cm^{-1} (Table 4) shows a 10 cm^{-1} decrease in frequency (Figure 6A), indicating electron density redistribution in the 4DMABN ligand core in the excited state.

Notice that a large change in the CN and Ph stretch frequencies of the 4DMABN ligand is expected if partial oxidation of the dimethyl amino moiety occurs. The observed spectral changes reveal that the state formed within the first 200 fs features an increase in the negative charge on the Re center and significant changes in electron distribution in the 4DMABN ligand. The resulting state can be viewed as having "mixed" triplet metal–ligand (DMABN) to ligand (bpy) charge transfer character (i.e., MLLCT).

Further, only small spectral changes occur over the first 50 ps for all the modes examined (Figure 6A), and no further changes are observed between 50 and 430 ps. Relaxation times of ca. 2.7 and ca. 18 ps are observed. Because both time components are much slower than the solvation time of DCM[40] and peaks shift to higher frequencies and narrow, the dynamics are assigned primarily to vibrational cooling of the complex, as with the **ReBN** complex. No further dynamics beyond 50 ps are found for **Re4DMABN** in DCM in the 430 ps time window for all vibrational peaks studied. Interestingly, despite the similarities in luminescence and transient absorption spectra and dynamics in the visible spectral region between **Re4DMABN** and its parent compound **ReBN**, the transient infrared spectra clearly

dx.doi.org/10.1021/jp409628e | J. Phys. Chem. B 2013, 117, 15903–15916

indicate significant electron density redistribution of the coordinated 4DMABN ligand.

Re4DMABN in MeOH/DCM: Equilibrium of LLCT and MLLCT States. The transient IR spectra of **Re4DMABN** in MeOH/DCM at small delay times (<1 ps) are similar to those in pure DCM (Figure 6B and Table S3, Supporting Information) for all modes studied. Instantaneous shifts to lower frequency of ν(CN) and ν_{ss}(Ph) suggest prompt formation of the MLLCT excited state. Notice that the width of the CN peak in the excited state in MeOH/DCM (ca. 44 cm^{-1}) is substantially larger than that in DCM (ca. 33 cm^{-1}), indicating increased inhomogeneity of CN environment in a more polar solvent.

The excited-state evolution of **Re4DMABN** in MeOH/DCM shows similarities with the behavior in DCM in the first few ps: the upward frequency shift and narrowing of the CO peaks, small growth of the CN peak all occur with a characteristic time of ca. 3 ps (Figure 6B). These dynamics clearly involve vibrational cooling but also can be influenced by solvation. The solvation dynamics in MeOH have two slow components, of 3.2 (30%) and 15.3 ps (26%);[40] the former can contribute to the observed spectral changes with a ca. 3 ps characteristic time. In addition to the relatively fast cooling−solvation process, a new process with a characteristic decay time of ca. 70 ps is found for all studied modes of **Re4DMABN** in the mixed MeOH/DCM solvent. This relaxation causes a downshift of all three CO frequencies, which for ν_{as2}(CO) is apparent from the increased absorbance at ca. 1910 cm^{-1}, accompanied by a bleach cancelation at ca. 1935 cm^{-1}, as well as by a substantial decrease of the ν_{ss}(CO) transition dipole, indicating that the changes are associated with an increase of the negative charge at the metal center. Concomitantly, the ν(CN) and ν_{ss}(Ph) peaks decrease by factors of 1.65 and 2.1, respectively. No new CN spectral region peaks were found as a result of the peak decay at 2190 cm^{-1}, which likely indicates that the new peak formed is weak and broad. The 70 ps decay of the peak at 1595 cm^{-1} leads to the formation of a weaker peak at 1555 cm^{-1} (Figure 6B, inset).

The 70 ps process is too slow to be associated with solvation or cooling; solvent facilitated structural rearrangements of the complex or electronic relaxation could be responsible for it. Only partial conversion of ca. 52% from the MLLCT state to the new state is found. Compared to the MLLCT state, the new state is characterized by increased electron density at Re, significant reduction of the ν_{ss}(Ph) frequency, and high electronic asymmetry for the three Re−N directions (large splitting of the two ν_{as}(CO) modes), suggesting substantial 4DMABN → bpy character (denoted as LLCT *vide infra*; Figure 8). On the basis of the amplitude of the changes (ca. 52%) of the ν_{ss}(Ph) amplitude, the LLCT state is slightly lower in energy than the MLLCT state that is well characterized in DCM. It is suggested that the LLCT state is responsible for the greatly enhanced excited state relaxation rate in the mixed solvent. Formation of the LLCT state is apparent in TRIR spectral changes of some vibrational modes (ν_{ss}(Ph)), while the other modes (CN) show only little changes.

Re3DMABN in DCM. Long-Lived ^{3}IL State Is Formed. Upon electronic excitation, the CO frequencies of **Re3DMABN** shift upward in accord with the formation of an MLCT state (Figure 7A). The frequency shift values, +70 (as_1), +30 (as_2), and +17 cm^{-1} (ss), are the largest among all three compounds (Table S2, Supporting Information), suggesting the preparation of a larger positive charge on the Re in **Re3DMABN**. The CN peak is shifted to lower frequencies upon excitation. The shift of −12 cm^{-1} (Figure 7A), which is larger than is found in **ReBN** (−10 cm^{-1}) but much smaller than is found in **Re4DMABN** (−50 cm^{-1}), suggests that the excited state in **Re3DMABN** has mostly MLCT character. Only a bleach signal is found for the ν_{ss}(Ph) mode at small time delays. Detailed analysis of the averaged transient spectra (Figure 7A inset, red line) indicates a bleach-peak cancelation on the low-frequency side of the peak, demonstrating that a new absorption peak is centered at ca. 1594 cm^{-1} (red arrow) and that the transition dipole of this mode in the excited state is reduced. Small frequency shifts of the ν_{ss}(Ph) and ν(CN) confirm that the initially prepared excited state is predominantly a MLCT (Re → bpy) state.

The excited state of **Re3DMABN** in DCM shows unique spectral changes occurring with a characteristic time of ca. 20 ps: the three CO peaks shift to lower frequencies by −26 cm^{-1} (as_1 and as_2) and −12 cm^{-1} (ss) with respect to the ground state frequencies. The modes ν(CN) and ν_{ss}(Ph) shift to lower frequencies by −127 and −66 cm^{-1}, respectively, indicating a large change of the 3DMABN charge distribution. The peak growth at 1535, 1920, 2029, and 2132 cm^{-1} occurs concomitantly with the decay at 1594, 1980, 2015, 2062, and 2250 cm^{-1} with a characteristic time of ca. 20 ps. What is the nature of this excited state? The downshift of the CO frequencies is formally consistent with the formation of a LLCT state. This would result in a net increase in electron density at Re, thereby increasing backbonding to the CO ligands, inducing a lowering in the CO stretching frequencies compared to the ground state. However, the CO peak structure indicates that the state formed features high symmetry with respect to the three facial CO ligands, which is apparent from the narrowness of ν_{ss}(CO) and an absence of splitting among the two ν_{as}(CO) modes. Notice that the formation of the (L → bpy) LLCT state would result in very different charges on the bpy and L ligands and lowering of the symmetry of the environment for the three CO groups. Thus, the data suggest that the final state formed in **Re3DMABN** is not LLCT in character. The observed spectral changes are consistent with evolution of the MLCT state to a ligand localized (IL) triplet excited state. In addition, for 4DMABN in hexane, the CN frequency in the triplet state is found to be 175 cm^{-1} below that in the ground state;[44] although no data are available for 3DMABN, formation of a strongly polarized (amine → CN) triplet state seems plausible. Thus, the excited state that decays to the ground state with a lifetime of 23 μs is assigned to a 3DMABN localized triplet state.

To clarify that the long-lived state is indeed a localized triplet state, we studied its quenching by pyrene, an aromatic hydrocarbon with a low-energy triplet state and a characteristic triplet visible absorption spectrum. Pyrene is found to be an effective quencher of the long-lived excited state of **Re3DMABN** with a second-order quenching rate constant of 4.9×10^9 M^{-1} s^{-1}. The transient absorption spectral changes observed in the quenching experiment (Figure S7, Supporting Information) illustrate disappearance of the absorbance of **Re3DMABN** and appearance of the characteristic pyrene triplet absorption transitions at 415 and 520 nm. This result supports the assignment of the thermally equilibrated excited state of **Re3DMABN** in DCM as a triplet state localized on the 3DMABN ligand.

The change in the CN bond order in the IL triplet state can be evaluated from the CN frequency shift. The CN mode shift

dx.doi.org/10.1021/jp409628e | J. Phys. Chem. B 2013, 117, 15903−15916

of 128 cm^{-1} corresponds to a relative change in the ν(CN) force constant with $k_{GS}/k_{ES} \sim 1.12$. Notice that the ratio of nitrile to imine (triple bond to double bond) force constants is approximately 1.8. Thus, the magnitude of the frequency shift in the IL triplet state represents a relatively small decrease in the CN bond order. The TRIR spectra of this complex very clearly illustrate complete conversion of the initially formed ^{3}MLCT state into a strongly polarized state localized on the 3DMABN ligand.

Re3DMABN in MeOH/DCM. Equilibrium of MLLCT and ^{3}IL States. The excited state prepared at 200 fs after **Re3DMABN** excitation in the mixed solvent is very similar to that in DCM, as indicated by a similarity of the frequency shifts of the CO and CN modes (Figure 7B and Table S2, Supporting Information). The ν(Ph) frequency is shifted to lower values by ca. 5−8 cm^{-1}, showing a ground state bleach cancelation at the low-frequency side. As in DCM, these spectral features are assigned to the formation of the Re → bpy MLCT state.

The spectral changes observed in the picosecond dynamics of the **Re3DMABN** excited state differ dramatically from those in pure DCM but occur with similar characteristic times of ca. 7 and 23 ps. Neither of the CO stretching modes shifts to lower frequency with time as in DCM. Instead, the CO peaks evolve further to higher frequencies with a characteristic time of 6−7 ps, which is assigned to solvation and vibrational cooling processes. The ν_{ss}(CO) peak in the excited state (at ∼2070 cm^{-1}) shows a typical vibrational Stokes-shift dynamics with a time constant of ca. 6 ps, similar to that reported by Lian and co-workers for a structurally related Re−carbonyl complex.[45,46] Surprisingly, the CN mode peak in the excited state evolves similarly to that in DCM. The initial absorption at 2244 cm^{-1} is reduced essentially to zero with a decay time of ca. 23 ps, while a new absorption grows in concomitantly at ca. 2125 cm^{-1}. The frequency shift in the mixed solvent (−135 cm^{-1}) is even larger than that in DCM (−127 cm^{-1}), indicating that the state formed is even more polar. Methanol absorption prevented measurements below 1560 cm^{-1}, so the frequency of the ν(Ph) mode in the relaxed state(s) could not be determined.

Thus, the dominant relaxed excited state for **Re3DMABN** in the mixed solvent at delays larger than 50 ps has less electron density at the Re than in the ground state (CO frequency upshift), an asymmetric facial environment for the CO groups (splitting of the two ν_{as}(CO) modes), and strong polarization of the 3DMABN ligand (large downshift of the ν(CN)). Because both bpy and L ligands are strongly affected in this state, we refer to it as an MLLCT state, although the degree of charge shift between the ligands remains unclear. The local L triplet state is also clearly seen in **Re3DMABN** in MeOH/DCM: a sharp peak at 2035 cm^{-1}, ν_{ss}(CO), and a broader peak at ca. 1915 cm^{-1}, ν_{as}(CO), are growing in with a time constant of ca. 24 ps, although the amplitudes of these spectral features are small. The similarity of the rising time with the characteristic time of the main MLLCT state formation indicates that the two states are in equilibrium. Using the amplitude of the peak at 2035 cm^{-1} in comparison to the bleach ν_{ss}(CO) peak and using the bleach-to-peak ratio in DCM as a reference, the contribution of the local triplet state in the MeOH/DCM mixture is estimated to be ca. 15%, which places the local triplet state ca. 400 cm^{-1} higher than the main triplet MLLCT state. Thus, increasing the polarity of the medium resulted in significant lowering of the ^{3}MLLCT state such that it becomes the dominant state but remains in equilibrium with the 3DMABN localized ^{3}IL state.

Excited State Assignments and Correlation with Relaxation Dynamics. The electronic states observed experimentally, and the rates of their interconversion, are summarized in Figure 8. The nature of the contributing excited

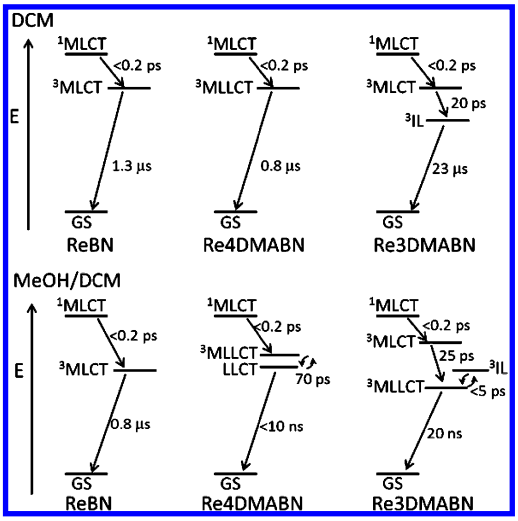

Figure 8. State diagrams for three complexes in different solvents including approximate transition times.

states in these compounds is better understood through comparison of the experimental nanosecond and ultrafast infrared data with the computational results. In addition to comparison of the vibrational frequency shifts with respect to the ground state, we analyzed how charges on different parts of the complexes (from Mulliken population analysis) change in the excited state. The dependence of the nature of the lowest energy triplet state on the solvent polarity was investigated theoretically by introducing solvent via a polarizable continuum model (PCM). To exaggerate the polarity influence and shift of the LLCT state to lower energies, the computations were performed in a medium of increased polarity with a dielectric constant of 81.

In the **ReBN** complex, formation of a pure ^{3}MLCT state is suggested by the experiments. DFT calculations show that the Mulliken electron density on bpy in the T1 state compared to the GS is increased by 0.26e (Table 5), while the charge at the BN ligand stays essentially unchanged (0.02e). The computed frequency shifts between T1 and GS are generally in agreement with the shifts found experimentally for the long-lived ^{3}MLCT state (Table S3, Supporting Information): in DCM, both asymmetric CO frequencies shift to higher values by 42 and 15 cm^{-1}, while ν(CN) shifted down by −9 cm^{-1}. In calculations of all three complexes, the symmetric CO stretching mode is shifted to lower frequencies, demonstrating imperfections in the computations; we will not discuss it therefore in detail. Relaxation of the MLCT state to the ground state occurs in approximately 1 μs in DCM and is somewhat shorter in the more polar solvent mixture.

Rapid formation of a MLLCT state in **Re4DMABN** is suggested by the TRIR experiments in both DCM and mixed solvent. Appearance of an additional state formed with 70 ps characteristic time from the MLLCT state is found in the mixed solvent; this state has features of a LLCT (L → bpy) state. The T1 state computed for **Re4DMABN** in DCM has a complex

dx.doi.org/10.1021/jp409628e | J. Phys. Chem. B 2013, 117, 15903−15916

electron-density redistribution, with substantial electron density depletion from the dimethyl aniline (−0.42e) and electron density gain at the bpy (0.67e; Table S5, Supporting Information). On the basis of the computed charge shifts, the MLLCT state has 64% LLCT (L → bpy) and 36% MLCT (Re → bpy) character. The computed vibrational frequency shifts match reasonably well with the experiment (Table S3, Supporting Information). For example, the ν(CN) and ν_{ss}(Ph) frequencies shift down by −47 and −19.5 cm^{-1}, compared to the experimental shifts of −46 and −10 cm^{-1}. The ν_{ss}(bpy) is shifted by −57 cm^{-1}, compared to −73 cm^{-1} in the experiment (peak at 1538 cm^{-1}, Figure 6A). For isolated 4DMABN molecules in methanol, hydrogen bonded intramolecular charge transfer (HICT) structures were identified in the excited state by Kwok and co-workers.[47] The H-bonding occurs at the cyano group and results in an additional ca. 20 cm^{-1} downshift of the CN frequency compared to that in the intramolecular charge transfer state. Not surprisingly, no second peak was found in the excited state of **Re4DMABN**, likely because the CN site is shielded by coordination to the rhenium atom.

The experimental results for **Re4DMABN** in the mixed solvent showed two states at equilibrium, one very similar to the MLLCT state characterized for **Re4DMABN** in DCM and another, denoted as LLCT, with substantial 4DMABN → bpy charge transfer character. To stabilize in calculations the LLCT state vs the MLLCT state, the **Re4DMABN** triplet excited states was computed in water described via the PCM model. The computed T1 state in water is found to have a large LLCT (4DMABN → bpy) contribution of ca. 81%. One asymmetric CO mode is shifted to lower frequency by −5 cm^{-1} with respect to their mean frequency in the GS (in agreement with the experimental peak at ca. 1910 cm^{-1}), while another is shifted to higher frequencies by 19 cm^{-1}. The CN frequency is shifted down by −41 cm^{-1}, which is very similar to that in the MLLCT state found in DCM (−47 cm^{-1}). These results suggest that the intensity decrease of the peak at 2190 cm^{-1} (Figure 6B) occurs due to reduction of the IR intensity of ν(CN) in the LLCT state and explains why no separate absorption peak was observed for the LLCT state. The computed shift of the ν_{ss}(Ph) frequency is −28 cm^{-1}, compared to the experimental shift of −47 cm^{-1}. Importantly, the ν_{ss}(Ph) absorption peak in the LLCT state does not overlap with that in the MLLCT state, providing a convenient observation frequency for evaluating the relative populations of the two states. The ν_{ss}(Ph) absorption at 1593 cm^{-1} decreases by ca. 2.1-fold with a rate constant of ca. 70 ps, which places the LLCT state slightly (150 cm^{-1}) below the MLLCT state. To summarize, the excited states computed for **Re4DMABN** in the two solvents characterize reasonably well the experimental observations (Figure 8).

The characteristic time to establish equilibrium among MLLCT and LLCT states, 70 ps, could be associated with the non-radiative decay process from the higher excited states to the triplet-ground state T1. For the **Re4DMABN** compound, the vertical excitation of energy between T1 and T2 is about 0.2 eV and that between S2 and T2 is approximately 0.5 eV. In addition, it was found in DCM solvent that there exists another local minimum whose energy is about 0.24 eV higher than that of the equilibrium geometry of the T1 state. Charge population analysis showed that this high-energy triplet minimum is a MLCT state, and single point calculations indicated it is not on the lowest triplet state. Therefore, it may correspond to an equilibrium structure on one of the triplet surfaces. According to perturbation theory, a small energy gap between the triplet states will result in the strong non-adiabatic interaction. Indeed, the nature of the T1 state global minimum, MLLCT, reflects this multireference nature of its electronic wave function. The relatively long equilibrating time could be attributed to the increased lifetime of the higher triplet excited state, which is caused by the stabilization of the charge separation due to the polar solvent. Upon UV excitation, the molecule is populated to the singlet MLCT state. Spin−orbit coupling will transfer the population onto the triplet manifold and, finally, the system will relax to the lowest triplet ground state through non-adiabatic transitions. In the course of this relaxation process, the CT nature changes from MLCT to MLLCT.

Transitions between different structural minima may also be responsible for the observed 70 ps time constant. The structures in the T1 states in the two solvents were compared, but no large changes were found. For example, a variation of the Re−N−C angle, anticipated due to stronger contribution of the quinoidal resonance 4DMABN structure in the polar solvent, was found to be too small (∼0.26°) to support the idea that such motion is responsible for the 70 ps process.

The excited state spectral changes observed experimentally for **Re3DMABN** in DCM are well described by the DFT calculations. A ^{3}MLCT state is rapidly formed in excited **Re3DMABN** in both DCM and mixed solvent. In DCM, a new state is formed with a 20 ps time constant, which has spectroscopic features consistent with being a local 3DMABN triplet state. The computed T1 state in DCM is predicted to be mostly a ^{3}IL state: The overall charge on the Re center and 3DMABN ligand changes only by −0.014 and 0.093, while the change of the charge at the dimethylamino and phenyl moieties together is +0.25, where the electron density is donated mostly to the cyano group (Table 5). The frequencies of both CO asymmetric stretches shift to lower frequencies by −14 and −20 cm^{-1}, compared to a ca. −25 cm^{-1} experimental shift, and the environment remains symmetric for the three facial carbonyls as the two frequencies remain close to each other with a 12 cm^{-1} separation, compared to the 10 cm^{-1} separation in the ground state. The CN stretching frequency is shifted by −128 cm^{-1}, compared to the experimental shift of −127 cm^{-1}. The computed shift of the ν_{ss}(Ph) mode is −75 cm^{-1}, compared to the observed −66 cm^{-1}. The overall match is good, which confirms that this excited state is mostly localized at the 3DMABN ligand. The T1 calculations of 3DMABN in water show very little differences from those in DCM. Essentially, the lowest state computed for **Re3DMABN** in water remains the ^{3}IL 3DMABN localized state, although it became slightly more polarized, which can be seen from an increase of the overall charge at the dimethylamino and phenyl moieties, which is +0.26, and from a larger CN frequency shift of −134 cm^{-1}. The experimentally observed MLLCT state is not computed as the lowest energy triplet state. The origin of the discrepancy is currently unclear.[48]

Assignment of excited states was reported in the literature for several Re−tricarbonyl complexes. The authors indicated formation of LLCT states in some of the systems. The assignment of the LLCT state formation was often based on behavior of CO frequencies, sometimes reinforced by lifetime measurements and/or DFT computations. For example, there are several reports where the downshift of the CO frequencies (both asymmetric and symmetric) with respect to the GS is

associated with formation of the LLCT state.[24,49] Our results indicate that the downshift of the CO frequencies alone does not necessarily indicate the formation of the LLCT state in Re complexes. For example, all of our data on **Re3DMABN** in DCM, which include TRIR data for many vibrational modes, excited state lifetime measurements, triplet state quenching experiments, and DFT calculations, unequivocally indicate that a ^{3}ILCT triplet state is formed, although all CO frequencies in this state shift to lower values. Certainly, the inclusion of a variety of vibrational labels in TRIR measurements implemented in this study increases greatly the confidence level of the assignment. For example, the CO frequency changes in the excited state of **Re4DMABN** in the mixed solvent are not conclusive of the LLCT state formation without considering ν(CN) and ν_{ss}(Ph) peak behaviors; the ν_{ss}(Ph) peak downshift by ca. 65 cm^{-1}, supported by DFT calculations, clearly indicates formation of the state with dominant LLCT character.

Quinoidal Resonance Structures of 4DMABN Lower the Charge-Transfer Extent in Re4DMABN Compared to Re3DMABN. The difference between the excited states of **Re3DMABN** and **Re4DMABN** can be related to the ability of the two DMABN ligands to form quinoidal charge-transfer resonance structures associated with partial or full charge transfer from the dimethylamino moiety to the nitrile moiety (Scheme S1, Supporting Information). Quinoidal charge transfer resonance structure is very favorable (has low energy) in 4DMABN but is unfavorable in 3DMABN because of the 1,3 substitution pattern. As a result, the 4DMABN ligand will likely behave as a single entity in all charge-shift reactions, so that the changes are delocalized over the whole ligand. In contrast, when the 3DMABN ligand is involved in electron donation, the electron density will mostly be drawn from its amino moiety. Figure 9 presents a qualitative three-state coupling diagram for

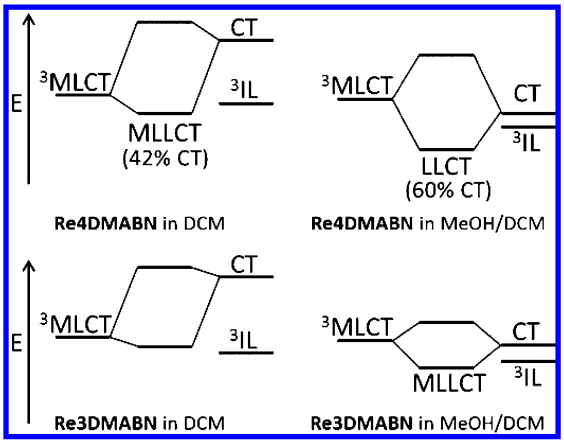

Figure 9. A three-state model describing charge-transfer extent in **Re4DMABN** and **Re3DMABN** in the two solvent systems.

Re4DMABN and **Re3DMABN** compounds in DCM and in a polar solvent. These states include a pure MLCT (Re → bpy) state characterized by an electron density shift from Re to bpy of ca. 0.2e (as in **ReBN**, Table 5), a formal full-electron CT (L → bpy) state, and an ideal fully L-localized triplet state, ^{3}IL. Proper mixing of these three states results in preparation of the characteristic states of the complex. The ideal MLCT and CT states are both associated with an increase of electron density on the bpy and therefore couple strongly. The coupling of the ^{3}IL state to the two other is assumed in comparison. Weak coupling of the ^{3}IL state to the MLCT and CT states is in agreement with experimental observations that the two states (MLLCT and ^{3}IL) are in equilibrium for **Re3DMABN** in MeOH/DCM (Figure 8). The MLCT and CT states are strongly coupled in **Re4DMABN** (large spatial overlap of the involved wave functions), enabled by the quinoidal resonance forms (Scheme S1, Supporting Information). In contrast, coupling in **Re3DMABN** is much weaker because of the larger distance for charge transfer (from amine to bpy) and the absence of bridge polarization because of the meta-conjugation pattern. In the model of Figure 9, the CT states of both compounds in DCM are placed substantially above the MLCT state in energy, as motivated by the experimental data. The ideal ^{3}IL state is placed lower than the CT state and just below the ideal MLCT state for both compounds in DCM. In polar solvent, the CT state shifts to substantially lower energies for both **Re4DMABN** and **Re3DMABN**, while the ^{3}IL state is affected little by the solvent polarity. Strong MLCT/CT coupling for **Re4DMABN** results in small shifts of the coupled states in DCM, because their initial energy gap is larger than the strength of the coupling.[50] The resulting low-energy state in DCM, labeled as MLLCT, has a dominant contribution of the MLCT state: the CT state contribution, evaluated as the loss of the charge density by the 4DMABN ligand, is ca. 42% (Table 5). As confirmed experimentally, this state is the lowest energy excited state in **Re4DMABN** in DCM. In the polar solvent, the ideal CT state is shifted below the ideal MLCT state, which results in much larger CT character of the state formed upon their mixing (60%, denoted as LLCT). Although the ideal CT state is now lower than the ideal MLCT, their strong coupling still results in formation of a mixed state with only partial CT character. An extremely large downshift is required to decouple the two states and obtain essentially a pure CT state in the complex; it is unlikely that any solvent is capable of shifting the ideal CT state in **Re4DMABN** that low. A similar situation is found for **Re3DMABN**, with the main difference being in the coupling strength of the ideal MLCT and CT states. Weaker coupling and off-resonant conditions result in only a small downshift of the mixed MLCT/CT state in DCM, which places it higher than the ^{3}IL state. In a polar solvent, the ideal CT state is in close resonance with the ideal MLCT state, resulting in a larger downshift of the mixed state, labeled as MLLCT, which is now very close to the ^{3}IL state; equilibrium between the two states is observed in the MeOH/DCM solvent (Figure 8). On the basis of the experimental observations, the lowest energy excited state in **Re3DMABN** in MeOH/DCM is denoted as MLLCT; it seems possible to drive this state lower and prepare a pure CT state if the polarity of the solvent is further increased or the CT state energy is lowered by structural alterations in the complex. Similar efforts with 4DMABN will give only partial success due to a strong MLCT/CT coupling. Satisfyingly, this three-state model describes well the majority of the experimental and computational observations.

CONCLUSIONS

Excited-state properties of a series of Re^I(bpy)(CO)$_3$L compounds were studied using time-resolved vibrational and electronic spectroscopy methods and DFT computations. The **Re4DMABN** and **Re3DMABN** complexes exhibit strongly solvent-dependent luminescence, having strong emission in dichloromethane (DCM) with microsecond lifetimes but being nearly completely quenched in the mixed MeOH/DCM solvent. Despite similarities in redox properties for **Re4DMABN** and **Re3DMABN** and in the excited-state lifetimes in

each solvent, the nature of the states observed in these systems is very different. For the **Re4DMABN** complex in DCM, essentially instantaneous formation of a long-lived (0.8 μs) triplet MLLCT excited state is found, while formation of the LLCT (4DMABN → bpy) state in close proximity to the MLLCT state is observed in the MeOH/DCM mixed solvent. The presence of this state, confirmed by DFT calculations, is believed to be responsible for drastic shortening of the excited state lifetime to less than 10 ns in the mixed solvent. An essentially pure MLCT excited state is formed within 0.2 ps of excitation of **Re3DMABN** in both solvent systems, although its dynamics are solvent dependent. In contrast to **Re4DMABN**, a long-lived (23 μs) intraligand triplet (^{3}IL, $^3(\pi-\pi^*)$) state is formed in **Re3DMABN** in DCM, while, in the mixed solvent, an equilibrium is observed between ^{3}IL and MLLCT states for **Re3DMABN**. The presence of the MLLCT state accounts for the excited state lifetime shortening by 3 orders of magnitude for **Re3DMABN** in the mixed solvent (20 ns). The set of excited states in these compounds appeared to be complex enough that their detailed characterization requires use of a combination of experimental methods, such as ps−ns TRIR, excited-state lifetime, and triplet state quenching measurements, as well as DFT computations. In addition, incorporation of multiple IR labels on different ligands in TRIR measurements is shown to be crucial in assessing the nature of the electronic states associated with charge localization, polarization, and transfer. A simple three-state model is proposed that well describes the origin of the drastic differences in the excited states involved in these two compounds. The model predicts that, even in a very polar solvent, the lowest energy state in **Re4DMABN** will not be a pure CT state. On the contrary, for **Re3DMABN**, it seems possible to generate an essentially pure CT state if the polarity of the solvent is increased or the CT state energy is lowered by structural changes in the complex.

■ ASSOCIATED CONTENT

Supporting Information

Detailed description on compound synthesis and characterization, X-ray crystallographic information, computational data, transient absorption in the visible for pyrene quenching of **Re3DMABN**, resonant structures of the compounds, and transient anisotropy data. This material is available free of charge via the Internet at http://pubs.acs.org.

■ AUTHOR INFORMATION

Corresponding Authors

*E-mail: russ@tulane.edu.
*E-mail: david.beratan@duke.edu.
*E-mail: irubtsov@tulane.edu.

Notes

The authors declare no competing financial interest.

■ ACKNOWLEDGMENTS

Support by the National Science Foundation (CHE-012357 to D.N.B. and CHE-1012371 to I.V.R.) and the U.S. Department of Energy, Office of Chemical Sciences (DE-FG-02-96ER14617 to R.H.S.) is gratefully acknowledged. Y.Y. is thankful for a fellowship from the IBM Corporation. The Louisiana Board of Regents (Grant LEQSF-(2002-03)-ENH-TR-67) and the National Science Foundation (CHE-1228232) are thanked for supporting the acquisition of Tulane University's X-ray diffractometers.

■ REFERENCES

(1) Barbara, P. F.; Jarzeba, W. Ultrafast Photochemical Intramolecular Charge and Excited State Solvation. *Adv. Photochem.* **1990**, *15*, 1−68.

(2) Gust, D.; Moore, T. A. *Intramolecular Photoinduced Electron-Transfer Reactions of Porphyrins*; Academic Press: San Diego, CA, 2000; pp 153−190.

(3) Meyer, T. J. Intramolecular Control of Excited State Electron and Energy Transfer. *Pure Appl. Chem.* **1990**, *62* (6), 1003−1009.

(4) Rettig, W. Photoinduced Charge Separation via Twisted Intramolecular Charge Transfer States. *Top. Curr. Chem.* **1994**, *169*, 253−299.

(5) Verhoeven, J. W. On the Role of Spin Correlation in the Formation, Decay, and Detection of Long-Lived, Intramolecular Charge-Transfer States. *J. Photochem. Photobiol., C* **2006**, *7* (1), 40−60.

(6) Skourtis, S. S.; Waldeck, D. H.; Beratan, D. N. Fluctuations in Biological and Bioinspired Electron-Transfer Reactions. *Annu. Rev. Phys. Chem.* **2010**, *61*, 461−485.

(7) Beratan, D. N.; Skourtis, S. S.; Balabin, I. A.; Balaeff, A.; Keinan, S.; Venkatramani, R.; Xiao, D. Steering Electrons on Moving Pathways. *Acc. Chem. Res.* **2009**, *42*, 1669−1678.

(8) Endicott, J. F.; Watzky, M. A.; Song, X.; Buranda, T. Observations Implicating Vibronic Coupling in Covalently Linked Transition Metal Electron Transfer Systems. *Coord. Chem. Rev.* **1997**, *159*, 295−323.

(9) Macqueen, D. B.; Perkins, T. A.; Schmehl, R. H.; Schanze, K. S. Photoinduced Intramolecular Electron Transfer in Rhenium(I) Chromophore-Quencher Complexes: Rate Dependence in the Inverted Region and the Use of a Rigid Organic Spacer. *Mol. Cryst. Liq. Cryst.* **1991**, *194*, 113−121.

(10) Blanco-Rodriguez, A. M.; Towrie, M.; Sykora, J.; Zalis, S.; Vlcek, A. Photoinduced Intramolecular Tryptophan Oxidation and Excited-State Behavior of $Re(L\text{-}AA)(CO)_3(\alpha\text{-diimine})]^{(+)}$ (L = Pyridine or Imidazole, AA = Tryptophan, Tyrosine, Phenylalanine). *Inorg. Chem.* **2011**, *50* (13), 6122−6134.

(11) El Nahhas, A.; Consani, C.; Blanco-Rodriguez, A. M.; Lancaster, K. M.; Braem, O.; Cannizzo, A.; Towrie, M.; Clark, I. P.; Zalis, S.; Chergui, M.; Vlcek, A., Jr. Ultrafast Excited-State Dynamics of Rhenium(I) Photosensitizers $[Re(Cl)(CO)_3(N,N)]$ and $[Re(imidazole)(CO)_3(N,N)]^+$: Diimine Effects. *Inorg. Chem.* **2011**, *50* (7), 2932−3943.

(12) Cannizzo, A.; Blanco-Rodriguez, A. M.; El Nahhas, A.; Sebera, J.; Zalis, S.; Vlcek, A., Jr.; Chergui, M. Femtosecond Fluorescence and Intersystem Crossing in Rhenium(I) Carbonyl-Bipyridine Complexes. *J. Am. Chem. Soc.* **2008**, *130* (28), 8967−8974.

(13) Liard, D. J.; Vlcek, A., Jr. Picosecond Dynamics of Photoinduced Interligand Electron Transfer in $Re(MQ^+)(CO)_3(dmb)]^{2+}$ (dmb = 4,4′-Dimethyl-2,2′-bipyridine, MQ^+ = N-Methyl-4,4′-bipyridinium). *Inorg. Chem.* **2000**, *39* (3), 485−490.

(14) Koutras, A.; Skea, J. E. F.; Stufkens, D. J.; Vlcek, A. Ligand-Dependent Excited State Behaviour of Re(I) and Ru(II) Carbonyl−Diimine Complexes. *Coord. Chem. Rev.* **1998**, *177* (53), 127−179.

(15) Bernhard, S.; Omberg, K. M.; Strouse, G. F.; Schoonover, J. R. Time-Resolved IR Studies of $[Re(LL)(CO)_4]^+$. *Inorg. Chem.* **2000**, *39* (14), 3107−3110.

(16) Gabrielsson, A.; Busby, M.; Matousek, P.; Towrie, M.; Hevia, E.; Cuesta, L.; Perez, J.; Zalis, S.; Vlcek, A., Jr. Electronic Structure and Excited States of Rhenium(I) Amido and Phosphido Carbonyl-Bipyridine Complexes Studied by Picosecond Time-Resolved IR Spectroscopy and DFT Calculations. *Inorg. Chem.* **2006**, *45* (24), 9789−9797.

(17) Kleverlaan, C. J.; Stufkens, D. J.; Clark, I. P.; George, M. W.; Turner, J. J.; Martino, D. M.; van Willigen, H.; Vlček, A. Photoinduced Radical Formation from the Complexes $[Re(R)(CO)_3(4,4'\text{-}Me_2\text{-}bpy)]$ (R = CH_3, CD_3, Et, iPr, Bz): A Nanosecond Time-Resolved Emission,

UV−Vis and IR Absorption, and FT-EPR Study. *J. Am. Chem. Soc.* **1998**, *120* (42), 10871−10879.
(18) Vlcek, A. Ultrafast Excited-State Processes in Re(I) Carbonyl-Diimine Complexes: From Excitation to Photochemistry. *Top. Organomet. Chem.* **2010**, *29*, 73−114.
(19) Dreyer, J.; Kummrow, A. Shedding Light on Excited-State Structures by Theoretical Analysis of Femtosecond Transient Infrared Spectra: Intramolecular Charge Transfer in 4-(Dimethylamino)-benzonitrile. *J. Am. Chem. Soc.* **2000**, *122* (11), 2577−2585.
(20) Liard, D. J.; Busby, M.; Matousek, P.; Towrie, M.; Vlček, A. Picosecond Relaxation of 3MLCT Excited States of [Re(Etpy)-$(CO)_3$(dmb)]$^+$ and [Re(Cl)$(CO)_3$(bpy)] as Revealed by Time-Resolved Resonance Raman, UV−vis, and IR Absorption Spectroscopy. *J. Phys. Chem. A* **2004**, *108* (13), 2363−2369.
(21) Vlcek, A.; Busby, M. Ultrafast Ligand-to-Ligand Electron and Energy Transfer in the Complexes fac-[Re^I(L)$(CO)_3$(bpy)]$^{n+}$. *Coord. Chem. Rev.* **2006**, *250* (13−14), 1755−1762.
(22) Bredenbeck, J.; Helbing, J.; Hamm, P. Labeling Vibrations by Light: Ultrafast Transient 2D-IR Spectroscopy Tracks Vibrational Modes during Photoinduced Charge Transfer. *J. Am. Chem. Soc.* **2004**, *126* (4), 990−991.
(23) Perkins, T. A.; Humer, W.; Netzel, T. L.; Schanze, K. S. Solvent-Induced Excited-State Quenching in a Chromophore Quencher Complex. *J. Phys. Chem.* **1990**, *94* (6), 2229−2232.
(24) Busby, M.; Matousek, P.; Towrie, M.; Clark, I. P.; Motevalli, M.; Hartl, F.; Vlcek, A., Jr. Rhenium-to-Benzoylpyridine and Rhenium-to-Bipyridine MLCT Excited States of fac-[Re(Cl)(4-benzoylpyridine)$_2$$(CO)_3$] and fac-[Re(4-benzoylpyridine)$(CO)_3$(bpy)]$^+$: A Time-Resolved Spectroscopic and Spectroelectrochemical Study. *Inorg. Chem.* **2004**, *43* (14), 4523−4530.
(25) Gribble, M. J.; Hunter, T. Hemophilus Aphrophilus Vertebral Osteomyelitis: A Case Report and Literature Review. *Diagn. Microbiol. Infect. Dis.* **1987**, *8* (3), 189−191.
(26) Hallett, A. J.; Pope, S. J. A. Towards Near-IR Emissive Rhenium Tricarbonyl Complexes: Synthesis and Characterisation of Unusual 2,2′-Biquinoline Complexes. *Inorg. Chem. Commun.* **2011**, *14* (10), 1606−1608.
(27) Liu, X.; Liu, J.; Pan, J.; Chen, R.; Na, Y.; Gao, W.; Sun, L. A Novel Ruthenium(II) Tris(bipyridine)-Zinc Porphyrin-Rhenium Carbonyl Triad: Synthesis and Optical Properties. *Tetrahedron* **2006**, *62* (15), 3674−3680.
(28) Lin, Z.; Lawrence, C. M.; Xiao, D.; Kireev, V. V.; Skourtis, S. S.; Sessler, J. L.; Beratan, D. N.; Rubtsov, I. V. Modulating Unimolecular Charge Transfer by Exciting Bridge Vibrations. *J. Am. Chem. Soc.* **2009**, *131* (50), 18060−18062.
(29) Frisch, M. J.; Trucks, G. W.; Schlegel, H. B.; Scuseria, G. E.; Robb, M. A.; Cheeseman, J. R.; Montgomery, J. A., Jr.; Vreven, T.; Kudin, K. N.; Burant, J. C.; et al. *Gaussian 09*, revision A.02; Gaussian, Inc.: Wallingford, CT, 2009.
(30) Perkins, T. A.; Humer, W.; Netzel, T. L.; Schanze, K. S. Solvent-Induced Excited-State Quenching in a Chromophore-Quencher Complex. *J. Phys. Chem.* **1990**, *94* (6), 2229−2232.
(31) Fraser, M. G.; Clark, C. A.; Horvath, R.; Lind, S. J.; Blackman, A. G.; Sun, X.-Z.; George, M. W.; Gordon, K. C. Complete Family of Mono-, Bi-, and Trinuclear $Re^I(CO)_3Cl$ Complexes of the Bridging Polypyridyl Ligand 2,3,8,9,14,15-Hexamethyl-5,6,11,12,17,18-hexaazatrinaphthalene: Syn/Anti Isomer Separation, Characterization, and Photophysics. *Inorg. Chem.* **2011**, *50* (13), 6093−6106.
(32) Striplin, D. R.; Crosby, G. A. Photophysical Investigations of Rhenium(I)Cl$(CO)_3$(phenanthroline) Complexes. *Coord. Chem. Rev.* **2001**, *211*, 163−175.
(33) Worl, L. A.; Duesing, R.; Chen, P.; Della Ciana, L.; Meyer, T. J. Photophysical Properties of Polypyridyl Carbonyl Complexes of Rhenium(I). *J. Chem. Soc., Dalton Trans.* **1991**, 849−858 (150th Anniv. Celebration Issue).
(34) Il'ichev, Y. V.; Kuhnle, W.; Zachariasse, K. A. Intramolecular Charge Transfer in Dual Fluorescent 4-(Dialkylamino)benzonitriles. Reaction Efficiency Enhancement by Increasing the Size of the Amino and Benzonitrile Subunits by Alkyl Substituents. *J. Phys. Chem. A* **1998**, *102* (28), 5670−5680.
(35) Blanco-Rodriguez, A. M.; Gabrielsson, A.; Motevalli, M.; Matousek, P.; Towrie, M.; Sebera, J.; Zalis, S.; Vlcek, A., Jr. Ligand-to-Diimine/Metal-to-Diimine Charge-Transfer Excited States of [Re(NCS)$(CO)_3$(alpha-diimine)] (alpha-diimine = 2,2′-bipyridine, di-iPr-N,N-1,4-diazabutadiene). A Spectroscopic and Computational Study. *J. Phys. Chem. A* **2005**, *109* (23), 5016−5025.
(36) Vlček, A.; Busby, M. Ultrafast Ligand-to-Ligand Electron and Energy Transfer in the Complexes fac-[Re^I(L)$(CO)_3$(bpy)]$^{n+}$. *Coord. Chem. Rev.* **2006**, *250* (13−14), 1755−1762.
(37) Dattelbaum, D. M.; Omberg, K. M.; Schoonover, J. R.; Martin, R. L.; Meyer, T. J. Application of Time-Resolved Infrared Spectroscopy to Electronic Structure in Metal-to-Ligand Charge-Transfer Excited States. *Inorg. Chem.* **2002**, *41* (23), 6071−6079.
(38) Hamm, P.; Ohline, S. M.; Zinth, W. Vibrational Cooling after Ultrafast Photoisomerization of Azobenzene Measured by Femtosecond Infrared Spectroscopy. *J. Chem. Phys.* **1997**, *106* (2), 519−529.
(39) Hamm, P.; Ohline, S.; Zurek, M.; Roschinger, T. Vibrational Cooling after Photoisomerization: First Application of a Novel Intramolecular Thermometer. *Laser Chem.* **1999**, *19* (1−4), 45−49.
(40) Horng, M. L.; Gardecki, J. A.; Papazyan, A.; Maroncelli, M. Subpicosecond Measurements of Polar Solvation Dynamics - Coumarin-153 Revisited. *J. Phys. Chem.* **1995**, *99* (48), 17311−17337.
(41) Lin, Z.; Keiffer, P.; Rubtsov, I. V. A Method for Determining Small Anharmonicity Values from 2DIR Spectra Using Thermally Induced Shifts of Frequencies of High-Frequency Modes. *J. Phys. Chem. B* **2011**, *115* (18), 5347−5353.
(42) Kasyanenko, V. M.; Lin, Z.; Rubtsov, G. I.; Donahue, J. P.; Rubtsov, I. V. Energy Transport via Coordination Bonds. *J. Chem. Phys.* **2009**, *131*, 154508/1−154508/12.
(43) Rubtsov, I. V. Energy Transport in Molecules Studied by Relaxation-Assisted 2DIR Spectroscopy. In *Ultrafast Infrared Vibrational Spectroscopy*; Fayer, M., Ed.; CRC Press: Boca Raton, FL, 2013; pp 333−359.
(44) Ma, C.; Kwok, W. M.; Matousek, P.; Parker, A. W.; Phillips, D.; Toner, W. T.; Towrie, M. Time-Resolved Study of the Triplet State of 4-Dimethylaminobenzonitrile (DMABN). *J. Phys. Chem. A* **2001**, *105* (19), 4648−4652.
(45) Anderson, N. A.; Lian, T. Ultrafast Electron Injection from Metal Polypyridyl Complexes to Metal-Oxide Nanocrystalline Thin Films. *Coord. Chem. Rev.* **2004**, *248* (13−14), 1231−1246.
(46) Anfuso, C. L.; Ricks, A. M.; Rodriguez-Cordoba, W.; Lian, T. Ultrafast Vibrational Relaxation Dynamics of a Rhenium Bipyridyl CO_2-Reduction Catalyst at a Au Electrode Surface Probed by Time-Resolved Vibrational Sum Frequency Generation Spectroscopy. *J. Phys. Chem. C* **2012**, *116* (50), 26377−26384.
(47) Kwok, W. M.; George, M. W.; Grills, D. C.; Ma, C. S.; Matousek, P.; Parker, A. W.; Phillips, D.; Toner, W. T.; Towrie, M. Direct Observation of a Hydrogen-Bonded Charge-Transfer State of 4-Dimethylaminobenzonitrile in Methanol by Time-Resolved IR Spectroscopy. *Angew. Chem., Int. Ed. Engl.* **2003**, *42* (16), 1826−1830.
(48) To characterize the T1 state of the **Re3DMABN** compound, besides B3LYP, three other functionals, including cam-B3LYP, LC-wPBE, and wB97x, were adopted to study its CT nature. These functionals have been shown to have better performance in the description of CT states. All of these functionals predicted that the nature of the T1 state is LLCT, which does not agree with the experimental observation. Additionally, the shifts of the vibrational frequencies are also inconsistent with the experiments.
(49) Lewis, J. D.; Towrie, M.; Moore, J. N. Ground- and Excited-State Infrared Spectra of an Azacrown-Substituted [(bpy)Re$(CO)_3$L]$^+$ Complex: Structure and Bonding in Ground and Excited States and Effects of Ba^{2+} Binding. *J. Phys. Chem. A* **2008**, *112* (17), 3852−3864.
(50) Davydov, A. S. *Theory of Molecular Excitons*; McGraw-Hill Book Co.: New York, 1962; p 174.